PROCEEDINGS OF SCIENCE

Inelastic cross section measurement in p-Pb collisions at 5.02 TeV with the CMS experiment

Melike Akbiyik, Sebastian Baur, Hauke Wöhrmann, Colin Baus*, **Igor Katkov, Ralf Ulrich**
Karlsruhe Institute of Technology
E-mail: colin.baus@kit.edu

for the CMS Collaboration

The inelastic cross section has been measured in proton-lead collisions at centre-of-mass energies per nucleon of 5.02 TeV at the LHC. Nuclear scaling effects play an important role in the simulation of cosmic ray interactions and are studied in collisions with lead nuclei. We present an overview of the related results published by the CMS Collaboration.

The 34th International Cosmic Ray Conference,
30 July- 6 August, 2015
The Hague, The Netherlands

*Speaker.

PoS(ICRC2015)440

1. Introduction

The inelastic cross section in hadronic collisions is a quantity that cannot be calculated in perturbative quantum chromodynamics (QCD) nor in any other theoretical framework based on first principles of QCD. Thus, it is one of the fundamental ingredient for Monte Carlo event generators. It is, however, possible to use the relation between elastic scattering, forward scattering amplitude and inelastic particle production to determine the inelastic cross section and at the same time multiple-scattering contributions. The fundamental argument behind this approach is the optical theorem. If this calculation is extended to include also nuclei, it is mainly the geometry of the nuclei that enters the calculation and the size of the nuclei that scales the cross section. The Glauber [1, 2] and Gribov-Regge [3] calculations can be used for this purpose. In such calculations also other effects influence the nuclear cross sections, which are non-geometric in their nature. These are foremost the effects of nucleon-correlations in the nuclei and inelastic intermediate states, related to low-mass single diffraction. For many applications these are typically neglected, while both can contribute on the level of 10 % to the calculations. Such effects are verified with measurements at lower energies [4, 5]. Precise experimental measurements of the proton-nucleus cross section at the LHC can help to shed light on the relative importance and the potential magnitude of these effects.

This is in particular relevant for cosmic ray applications, where such data are fundamental ingredients for the hadronic interaction models used to simulate extensive air showers. Furthermore, an extended Glauber calculation including inelastic screening is used for example by the Pierre Auger Collaboration to determine pp cross sections from the measured proton-air production cross section [6].

2. Experimental setup and data analysis

The central part of the CMS experiment is the 3.8 T solenoid magnet, which contains the silicon tracker, electromagnetic calorimeter and also most parts of the hadronic calorimeter. A general description of the CMS detector can be found elsewhere [7].

This analysis [8] uses proton-lead collision data collected in the first weeks of 2013 by the CMS experiment. The trigger decision is based on dedicated capacitive beam pickup detectors (BPTX). These detectors are installed ± 175 m away from the interaction point and detect the presence of particle bunches from the beam. The trigger configuration required the presence of the BPTX detectors of both beams, which does not influence the trigger decision based on any kind of observed particle production activity. This is typically called a "zero bias" condition. To measure the contribution from beam-gas collisions and electronic noise backgrounds, also data with the presence of exactly one or none of the BPTX detectors is studied.

Inelastic collisions are tagged using the hadronic forward (HF) detector [9] that covers the pseudorapidity interval $3 < |\eta| < 5$ with one calorimeter on either side of the interaction region. The calorimeter is composed of quartz fibres in a steel matrix with a 0.175×0.175 segmentation in the azimuthal angle, ϕ, and pseudorapidity, η. The quartz fibres pick up the Cherenkov light produced by the charged component of the showers. This light is then measured by photodetector tubes. The hadronic and electromagnetic signal of each segment is combined to form a *tower* signal. In the following, the single highest signal for a tower in the HF calorimeters is used for the

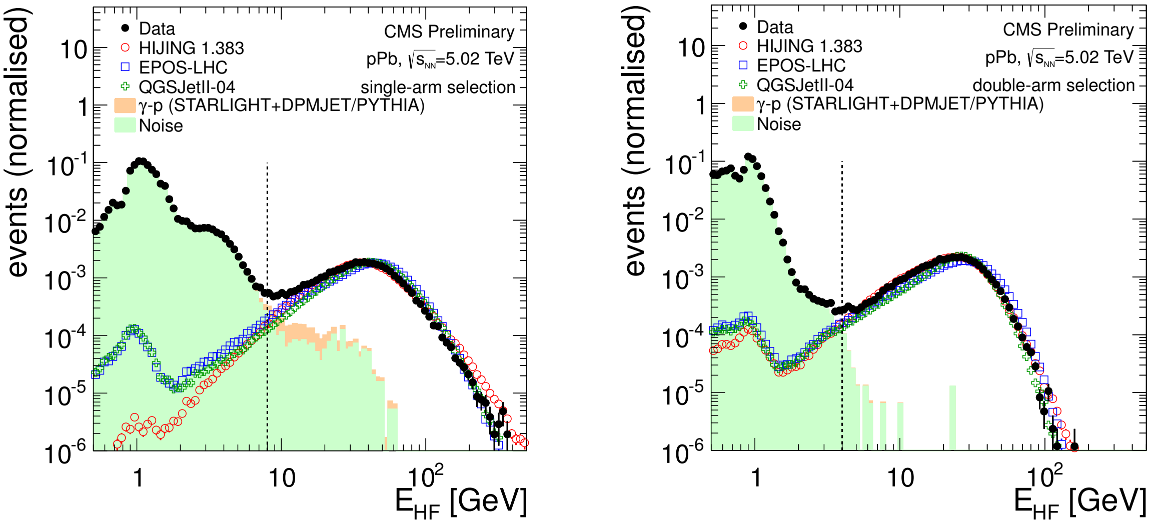

Figure 1: Distribution of E_{HF}. The noise rate (random trigger with empty bunch crossings) is matched to the zero bias trigger rate. The average of γp simulated with STARLIGHT+DPMJET and STARLIGHT+PYTHIA is added to the background as well. Three hadronic interaction models (EPOS, HIJING, and QGSJET) are also shown. These models are normalised to the number of zero bias events above 10 GeV, where the contribution from the background is low. The vertical lines represent the threshold energies used in this analysis.

analysis. The luminosity of the beams was measured with two Van-der-Meer scans, one for each beam configuration. The analysis is performed for two different event selections, both relying on the HF tower with the largest measured energy deposit:

- The **single-arm event selection** relies on a single sided HF event selection. This has the largest possible acceptance for inelastic events. In particular it has a high acceptance of single-diffractive events. At the same time, it also has an increased acceptance for photo-nuclear events. Furthermore, the absence of a coincidence requirement leads to an increased noise level, which requires larger values for the event selection energy threshold.

- The **double-arm event selection** is based on the coincidence requirement of both HF detectors. This reduces the noise rate and allows for smaller values of energy thresholds for the event selection. The coincidence requirement also removes efficiently photo-nuclear events. However, also a fraction of the single-diffractive events is removed. Hence, the acceptance towards inelastic collisions is reduced in the double-arm case.

Defining the highest energy in a tower of the HF calorimeter positioned at positive (negative) rapidity, $E_{\mathrm{HF+}}$ ($E_{\mathrm{HF-}}$), we define the following variable:

$$E_{\mathrm{HF}} = \begin{cases} \max(\mathrm{E}_{\mathrm{HF+}}, \mathrm{E}_{\mathrm{HF-}}) & \text{(single-arm selection)} \\ \min(\mathrm{E}_{\mathrm{HF+}}, \mathrm{E}_{\mathrm{HF-}}) & \text{(double-arm selection)}\,. \end{cases} \tag{2.1}$$

In Fig. 1 the distribution of E_{HF} is shown for both, the single- and double-arm selection. The threshold on E_{HF} is chosen to yield a similar magnitude of the correction for background noise and the limited acceptance to hadronic inelastic events. The selected thresholds for the single-arm and double-arm event selection are 8 GeV and 4 GeV, respectively.

Collisions mediated by the exchange of photons are subtracted from the measurement. For this purpose the STARLIGHT programme [10] combined either with DPMJET-III [11] or PYTHIA6 [12] have been used to generate photon-proton interactions.

The acceptance correction to estimate the loss of inelastic events invisible to the analysis is performed with the interaction models, which have diffractive final states fully implemented. This is not the case for HIJING [13] and DPMJET, and thus they can not be used for this purpose. Only EPOS [14] and QGSJetII [15] are used.

The results of the measurement is presented on various levels of corrections. First, the untreated *visible* cross section is given, which includes the contribution of electromagnetic collisions. In a next step, the electromagnetic contribution is subtracted, and the *visible hadronic* cross section is given. Only in the last step, the limited acceptance of CMS is also corrected for and the *inelastic* cross section (without the quasi-elastic contribution) is presented.

3. Results and conclusion

This final result for the hadronic inelastic cross section of p-Pb collisions at a centre-of-mass energy per nucleon of 5.02 TeV is determined to be

$$\sigma_{\mathrm{inel}} = 2.061 \pm 0.003(\mathrm{stat.}) \pm 0.039(\mathrm{syst.}) \pm 0.072(\mathrm{lumi.})\,\mathrm{b}\ . \tag{3.1}$$

The uncertainty is dominated by the precision of the luminosity scale. For a complete overview of the systematic uncertainties see Tab. 1. In Tab. 2 all cross section results of the analysis are summarized. It is interesting that these are the largest values of cross sections measured at LHC so far. In Fig. 2 the cross section data is shown on all levels of corrections. QGSJetII tends to predict slightly large values.

Table 1: Systematic uncertainties on σ_{inel} for two event selection methods.

Source of uncertainty		Single-arm	Double-arm
Luminosity measurement		3.5%	3.5%
Pileup uncertainty		<0.1%	<0.1%
Extrapolation $\sigma_{\mathrm{vis}}^{\mathrm{had}} \rightarrow \sigma_{\mathrm{inel}}$	Model difference	0.5%	1.6%
	optimised σ_{diff}	1.5%	2.0%
Photo-nuclear correction		0.2%	<0.1%
Modelling uncertainty		1.7%	0.8%
Event selection		0.6%	0.2%
Noise subtraction		1.2%	0.2%
Total without σ_{lumi}		2.7%	2.7%
Total with σ_{lumi}		4.4%	4.4%
Both selections combined		4.0%	

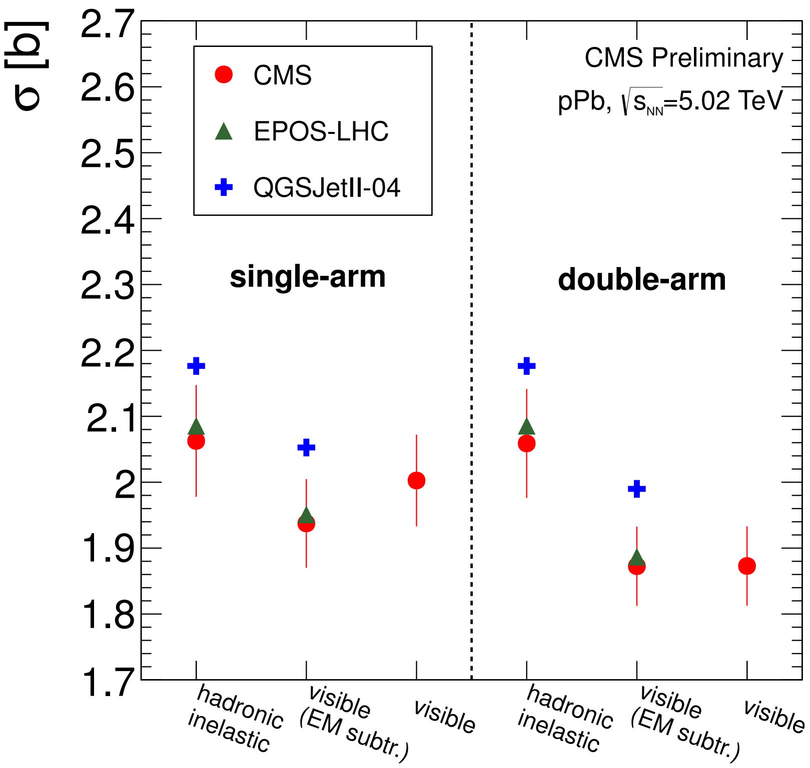

Figure 2: Overview of all cross section measurements performed in this analysis. The data is compared with model predictions.

The values of the pPb hadronic inelastic cross section measured as a function of the nucleon-nucleon centre-of-mass energy are shown in Fig. 3. The lowest energy data correspond to the absorption cross section measured at IHEP [16] and FNAL [17]. The intermediate-energy values up to 3.5 TeV correspond to cosmic ray data on a fixed lead target [18]. The model predictions reproduce the experimental data with good accuracy.

The measured hadronic inelastic cross section is compared to the standard Glauber calculation with 70 mb as input for the proton-proton cross section. The proton-proton cross section was derived by the COMPETE parametrisation [19] including the TOTEM measurement at 7 TeV [20]. With this as input, it follows a prediction of the Glauber theory of $\sigma_{\text{inel}} = 2.13 \pm 0.04\,\text{b}$ which is compatible with the result of this analysis. This points to the fact that screening corrections and anti-screening effects are similar in magnitude (but opposite in sign) for pPb collisions at 5.02 TeV.

Table 2: The visible cross section (noise and pileup corrected), visible hadronic cross section (as visible but without photon-proton contribution) and hadronic inelastic cross section (as hadronic but extrapolated to ideal acceptance) obtained by the two different event selections.

Selection	σ_{vis} (b)	$\sigma_{\text{vis}}^{\text{had}}$ (b)	σ_{inel} (b)
$E_{\text{HF}} > 8$ GeV (single-arm)	2.003	1.938	2.063
$E_{\text{HF}} > 4$ GeV (double-arm)	1.873	1.873	2.059

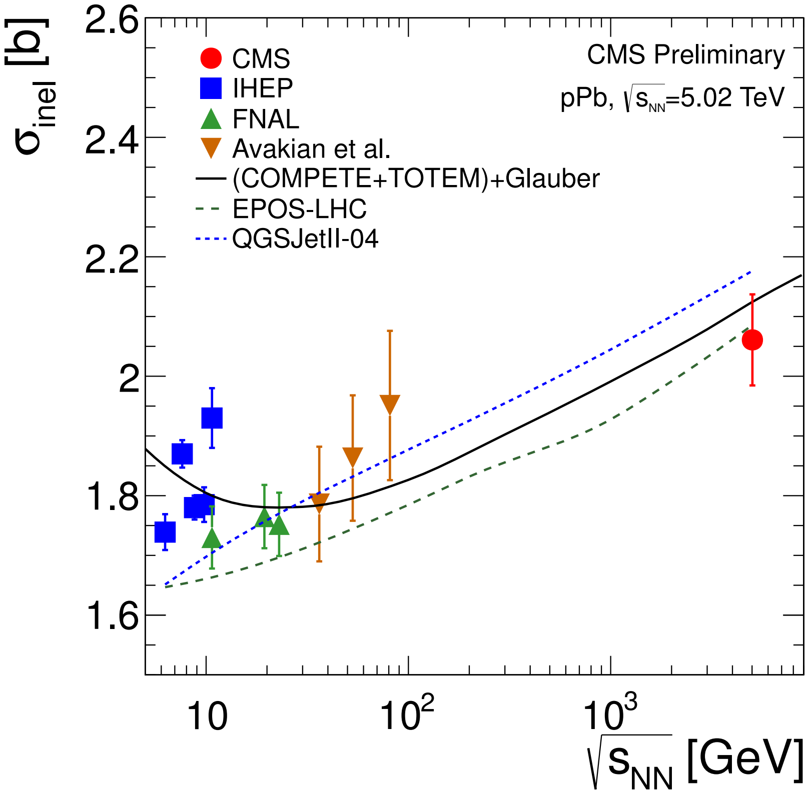

Figure 3: The energy dependence of the proton-lead cross section measurements. CMS contributes the by far highest energy data. For references see [16, 17, 18].

Thus, the Glauber calculation gives a reasonable result within the precision of the measurement. Furthermore, the other model predictions are also compatible with the measurements given the experimental uncertainties.

References

[1] R. Glauber, *Cross-sections in deuterium at high-energies*, Phys. Rev. **100** (1955) 242.

[2] R. Glauber and G. Matthiae, *High-energy scattering of protons by nuclei*, Nucl. Phys. B **21** (1970) 135.

[3] V. Gribov, *Glauber corrections and the interaction between high-energy hadrons and nuclei*, Sov. Phys. JETP **29** (1969) 483.

[4] Ciofi degli Atti et al., *Number of Collisions in the Glauber Model and Beyond* **84** (2011) 025205.

[5] M. Alvioli et al., *Nucleon momentum distributions, their spin-isospin dependence and short-range correlations*, Phys. Rev. C **87** (2013) 034603.

[6] The Pierre Auger Collaboration, *Measurement of the proton-air cross-section at $\sqrt{s}$=57 TeV with the Pierre Auger Observatory*, Phys. Rev. Lett. **109** (2012) 062002.

[7] S. Chatrchyan et al., CMS Collaboration, *The CMS experiment at the CERN LHC*, JINST **3** (2008) S08004.

[8] S. Chatrchyan et al., CMS Collaboration, *Measurement of the inelastic hadronic cross section in pPb collisions at $\sqrt{s}$=5.02 TeV*, CMS-PAS-FSQ-13-006 (2013) `https://cds.cern.ch/record/2010485`.

[9] J. Merlo et al., *CMS hadronic forward calorimeter*, Nucl. Phys. Proc. Suppl. B **61** (1998) 41.

[10] O. Djuvsland and J. Nystrand, *Single and double photonuclear excitations in Pb+Pb collisions at $\sqrt{s_{NN}} = 2.76$ TeV at the CERN Large Hadron Collider*, Phys. Rev. C **83** (2011) 041901.

[11] F. Bopp, J. Ranft, R. Engel, S. Roesler, *Antiparticle to particle production ratios in hadron-hadron and d-Au collisions in the DPMJET-III Monte Carlo*, Phys. Rev. C **77** (2008) 014904.

[12] T. Sjostrand, S. Mrenna, P. Skands, *A brief introduction to PYTHIA 8.1*, Comput. Phys. Commun. **178** (2008) 852.

[13] X. Wang and M. Gyulassy, *HIJING: A Monte Carlo model for multiple jet production in p p, p A and A A collisions*, Phys. Rev. D **44** (1991) 3501.

[14] K. Werner et al. *Parton ladder splitting and the rapidity dependence of transverse momentum spectra in deuteron-gold collisions at RHIC*, Phys. Rev. C **74** (2006) 044902.

[15] S. Ostapchenko, *Air shower calculations with QGSJET-II: Effects of Pomeron loops*, Nucl. Phys. Proc. Suppl. **196** (2009) 90.

[16] S. Denisov at al., *Absorption cross-sections for pions, kaons, protons and anti-protons on complex nuclei in the 6-GeV/c to 60-GeV/c momentum range*, Nucl. Phys. B **61** (1973) 62.

[17] A. Carroll et al., *Absorption Cross-Sections of $\pi^{\pm}$, $K^{\pm}$, p and anti-p on Nuclei Between 60 GeV/c and 280 GeV/c*, Phys. Lett. B **80** (1979) 319.

[18] V. Avakian et al., *Determining inelastic interaction cross-sections for nucleons and pions incident on carbon and lead nuclei at 0.5 TeV - 5 TeV*, Bull. Russ. Acad. Sci. Phys. **50N11** (1986) 4.

[19] B. Nicolescu et al., *Analytic parametrizations of the nonperturbative pomeron and QCD inspired models*, hep-ph/0110170 (2001) 265.

[20] G. Antchev et al., TOTEM Collaboration, *Luminosity-independent measurements of total, elastic and inelastic cross-sections at $\sqrt{s} = 7$ TeV*, Europhys. Lett. **101** (2013) 21004.

PoS(ICRC2015)440